RIPK1 activates distinct gasdermins in macrophages and neutrophils upon pathogen blockade of innate immune signaling

Kaiwen W. Chen[a,b,1,2], Benjamin Demarco[a,1], Saray Ramos[a], Rosalie Heilig[a], Michiel Goris[a], James P. Grayczyk[c], Charles-Antoine Assenmacher[c], Enrico Radaelli[c], Leonel D. Joannas[d,e], Jorge Henao-Mejia[d,e,f], Fabienne Tacchini-Cottier[a], Igor E. Brodsky[c,e], and Petr Broz[a,2]

[a]Department of Biochemistry, University of Lausanne, CH-1066 Epalinges, Switzerland; [b]Immunology Translational Research Programme and Department of Microbiology and Immunology, Yong Loo Lin School of Medicine, National University of Singapore, Singapore 117456; [c]Department of Pathobiology, University of Pennsylvania School of Veterinary Medicine, Philadelphia, PA 19104; [d]Department of Pathology and Laboratory Medicine, University of Pennsylvania, Philadelphia, PA 19104; [e]Institue for Immunology, University of Pennsylvania Perelman School of Medicine, Philadelphia, PA 19104; and [f]Division of Protective Immunity, Department of Pathology and Laboratory Medicine, Children's Hospital of Philadelphia, University of Pennsylvania, Philadelphia, PA 19104

Edited by Li Zhang, Department of Microbiology and Immunology, Weill Cornell Medicine, New York, NY, and accepted by Editorial Board Member Carl F. Nathan May 27, 2021 (received for review January 20, 2021)

Injection of effector proteins to block host innate immune signaling is a common strategy used by many pathogenic organisms to establish an infection. For example, pathogenic *Yersinia* species inject the acetyltransferase YopJ into target cells to inhibit NF-κB and MAPK signaling. To counteract this, detection of YopJ activity in myeloid cells promotes the assembly of a RIPK1–caspase-8 death–inducing platform that confers antibacterial defense. While recent studies revealed that caspase-8 cleaves the pore-forming protein gasdermin D to trigger pyroptosis in macrophages, whether RIPK1 activates additional substrates downstream of caspase-8 to promote host defense is unclear. Here, we report that the related gasdermin family member gasdermin E (GSDME) is activated upon detection of YopJ activity in a RIPK1 kinase–dependent manner. Specifically, GSDME promotes neutrophil pyroptosis and IL-1β release, which is critical for anti-*Yersinia* defense. During in vivo infection, IL-1β neutralization increases bacterial burden in wild-type but not *Gsdme*-deficient mice. Thus, our study establishes GSDME as an important mediator that counteracts pathogen blockade of innate immune signaling.

gasdermin | *Yersinia* | RIPK1 | neutrophils | caspases

Gasdermins are a family of recently described pore-forming proteins and are emerging as key drivers of cell death and inflammation. Gasdermins comprise a cytotoxic N-terminal domain connected to an inhibitory carboxyl-terminal domain and are activated upon proteolytic cleavage (1, 2). This cleavage event releases the cytotoxic N-terminal fragment, which creates membrane pores and triggers a form of lytic cell death called pyroptosis (3–6). Gasdermin D (GSDMD) is arguably the best characterized family member to date and is activated upon proteolysis by caspase-1, 4, 5, 8, and 11 and serine proteases (7–14). Active GSDMD promotes host defense by eliminating the replicating niche of intracellular pathogens (15) and inducing the extrusion of antimicrobial neutrophil extracellular traps (NETs) (16). In addition, GSDMD pores act as a conduit for bioactive IL-1β release (17–19), a potent proinflammatory cytokine that similarly requires proteolytic cleavage by caspase-1 or -8 to gain biological activity (20). By contrast, gasdermin E (GSMDE [also known as DFNA5]) is activated by apoptotic caspase-3 and 7 and granzyme B, which drives tumor cell pyroptosis and anti-tumor immunity (21–23). The physiological function of GSDME in primary immune cells and its potential role in host defense remain unresolved and have not been reported.

Pathogenic *Yersinia* are a group of Gram-negative extracellular bacteria that causes disease ranging from gastroenteritis (*Yersinia pseudotuberculosis*) to plague (*Y. pestis*). A major mechanism by which pathogenic *Yersinia* establish systemic infection is by injecting the effector protein YopJ, an acetyltransferase that blocks transforming growth factor beta-activated kinase 1 (TAK1), to inhibit host innate immune signaling and proinflammatory cytokine production (24). To counteract this, detection of YopJ activity by myeloid cells induces the assembly of a cytoplasmic death–inducing complex that comprises receptor-interacting serine/threonine protein kinase 1 (RIPK1), fas-associated protein with death domain, and caspase-8 (24–26). During in vivo infection, RIPK1/caspase-8–dependent cell death in myeloid cells restricts bacterial dissemination and replication at distal sites by inducing proinflammatory cytokine production from uninfected bystander cells (24). More recently, GSDMD was identified as a caspase-8 substrate during *Yersinia* infection that drives antimicrobial defense in vivo (11, 12, 27). However, whether RIPK1 activates additional substrates to restrict *Yersinia* infection is unclear and is a focus of this study. Here, we identify GSDME as a substrate activated downstream

Significance

Pathogenic bacteria subvert host-defense mechanisms by injecting effector proteins into target cells to inhibit NF-κB and MAPK signaling. Detection of such effector proteins, such as YopJ from pathogenic *Yersinia*, activates RIPK1 and caspase-8–dependent cell death that promotes antibacterial defense. While recent studies demonstrate that caspase-8 cleaves the pore-forming protein gasdermin D to promote anti-*Yersinia* defense, whether RIPK1 activates other substrates is unclear. Here, we demonstrate that RIPK1 activates gasdermin D in macrophages and the related gasdermin E in neutrophils to promote host defense. Neutralization of IL-1β in vivo promoted host susceptibility to *Yersinia* infection in wild-type, but not *Gsdme*$^{-/-}$, animals, revealing an unexpected role for gasdermin E in IL-1β secretion during bacterial infection.

Author contributions: K.W.C., B.D., and P.B. designed research; K.W.C., B.D., S.R., R.H., M.G., J.P.G., C.-A.A., and E.R. performed research; L.D.J., J.H.-M., F.T.-C., I.E.B., and P.B. contributed new reagents/analytic tools; K.W.C., B.D., S.R., R.H., M.G., J.P.G., F.T.-C., I.E.B., and P.B. analyzed data; and K.W.C. and P.B. wrote the paper.

The authors declare no competing interest.

This article is a PNAS Direct Submission. L.Z. is a guest editor invited by the Editorial Board.

Published under the PNAS license.

[1]K.W.C. and B.D. contributed equally to this work.

[2]To whom correspondence may be addressed. Email: kaiwen.chen@nus.edu.sg or petr.broz@unil.ch.

This article contains supporting information online at https://www.pnas.org/lookup/suppl/doi:10.1073/pnas.2101189118/-/DCSupplemental.

Published July 6, 2021.

of RIPK1 that confers host resistance against *Yersinia*. *Gsdme*-deficient mice failed to control bacterial replication in the spleen and liver and consequently are more susceptible to *Yersinia* infection than wild-type (WT) animals. Mechanistically, our data reveal that RIPK1 promotes caspase-3–dependent GSDME activation and IL-1β release in neutrophils, but not macrophages. Neutralization of IL-1β impaired bacterial clearance in WT, but not $Gsdme^{-/-}$, animals, indicating that IL-1β is mainly secreted through GSDME pores during *Yersinia* challenge in vivo.

RIPK1 Promotes GSDMD-Dependent and -Independent Antimicrobial Response.

We and others recently demonstrated that RIPK1-dependent GSDMD activation promotes macrophage pyroptosis and host defense against pathogenic *Yersinia* infection in vivo (11, 12, 27); however, whether RIPK1 activates other substrates to promote anti-*Yersinia* defense is unclear. To investigate this possibility, we challenged WT, $Gsdmd^{-/-}$, and $Ripk1^{D138N/D138N}$ "kinase-dead" mice (hereafter referred as $Ripk1^{KD}$) with *Yersinia pseudotuberculosis* (*Yptb*) and monitored their survival. In agreement with a previous report (24), RIPK1 kinase activity is critical for anti-*Yersinia* defense, as $Ripk1^{KD}$ mice exhibited 100% mortality within 7 d of infection, whereas more than 70% of WT animals survived 14 d postinfection (Fig. 1*A*). Surprisingly, we observed that *Gsdmd* deficiency does not fully recapitulate the susceptibility of $Ripk1^{KD}$ mice to *Yptb* infection (Fig. 1*A*), indicating that RIPK1 kinase activity activates additional unidentified substrates to confer anti-*Yersinia* defense. Since RIPK1 kinase activity promotes caspase-8–dependent apoptotic caspase activation (28) and apoptotic caspases-3/7 cleave GSDME (21, 23), we investigated whether GSDME drives antibacterial defense. Indeed, $Gsdme^{-/-}$ mice were significantly more susceptible to *Yptb* infection compared to WT controls (Fig. 1*B*), and significantly more bacteria were recovered from the spleen and liver of $Gsdme^{-/-}$ mice compared to WT controls (Fig. 1 *C* and *D*). In contrast, comparable bacteria were recovered from mesenteric lymph nodes (MLNs) and Peyer's patches (PP) of WT and $Gsdme^{-/-}$ mice (Fig. 1 *E* and *F*), indicating that GSDME primarily functions to prevent *Yptb* dissemination and replication at distal sites. These observations are consistent with the reported function of RIPK1 in myeloid cells during *Yersinia* infection (24). Next, to determine whether the combined function of GSDMD and GSDME accounts for RIPK1-driven antimicrobial defense, we orally challenged WT, $Ripk1^{KD}$ and $Gsdmd^{-/-}Gsdme^{-/-}$ mice with *Yptb*. Interestingly, while splenic bacterial load was comparable between $Ripk1^{KD}$ and $Gsdmd^{-/-}Gsdme^{-/-}$ mice (Fig. 1*G*), we consistently recovered more bacteria in the liver of $Ripk1^{KD}$ compared to $Gsdmd^{-/-}Gsdme^{-/-}$ mice (Fig. 1*H*), suggesting that GSDMD and GSDME activation are not the only mechanism by which RIPK1 kinase promotes antimicrobial defense in the liver. However, $Ripk1^{KD}$ and $Gsdmd^{-/-}Gsdme^{-/-}$ animals displayed comparable susceptibility to *Yptb* infection over 12 d (Fig. 1*I*), indicating that GSDMD and GSDME are the key substrates that are activated downstream of RIPK1 during *Yersinia* infection.

GSDME Is Dispensable for Macrophage Pyroptosis or Cytokine Secretion upon *Yptb* Infection.

Because RIPK1 kinase activity drives anti-*Yersinia* defense through the myeloid compartment (24), and *Yersinia* infection promotes RIPK1-dependent cell death in macrophages (11, 12, 24–26), we next focused our studies using bone marrow–derived macrophages (BMDMs). Consistent with previous reports (11, 12, 27), *Yptb* infection triggered robust processing of full-length GSDMD into its active p30 and inactive p20 fragment (Fig. 2*A*), and corresponding GSDMD-dependent pyroptosis in WT macrophages (Fig. 2*B*). Interestingly, while GSDME was completely processed into its active p30 fragment (Fig. 2*A*), lactate dehydrogenase (LDH) release between WT and $Gsdme^{-/-}$ BMDMs was indistinguishable (Fig. 2*B*). *Gsdme* deficiency did not further reduce LDH release in $Gsdmd^{-/-}$ macrophages (Fig. 2*B*), indicating that GSDME is dispensable for macrophage pyroptosis in both WT and $Gsdmd^{-/-}$ macrophages during *Yptb* infection. Gasdermin-dependent pyroptosis is often tightly coupled with the release of mature IL-1β.

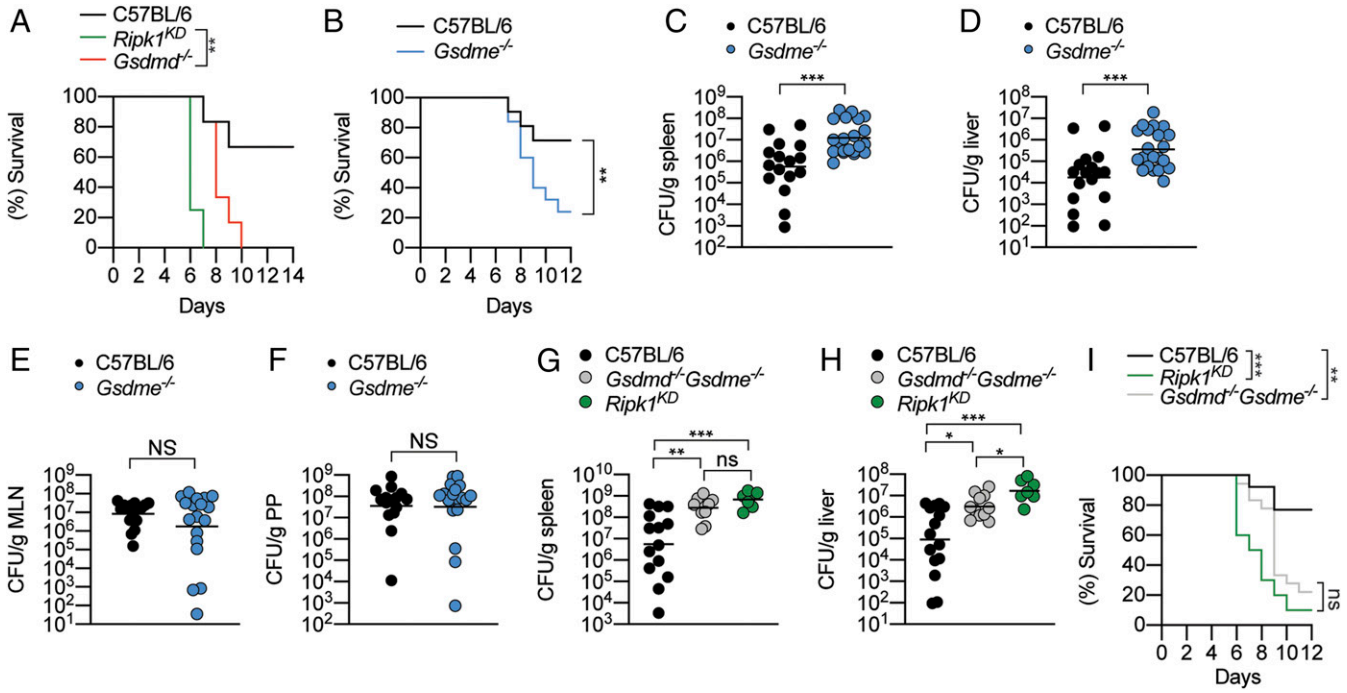

Fig. 1. GSDME promotes host defense against *Yptb* infection. (*A–I*) Mice were challenged with 2×10^8 CFU *Yptb*. (*C–H*) Bacterial load in the (*C* and *G*) spleen, (*D* and *H*) liver, (*E*) MLNs, and (*F*) PP were quantified at 5 d postinfection. (*C–H*) Data are geometric mean pooled from two independent experiments. Survival curves are (*A*) representative of two experiments or pooled from (*B*) three or (*I*) two independent experiments. $*P < 0.05$, $**P < 0.01$, or $***P < 0.001$.

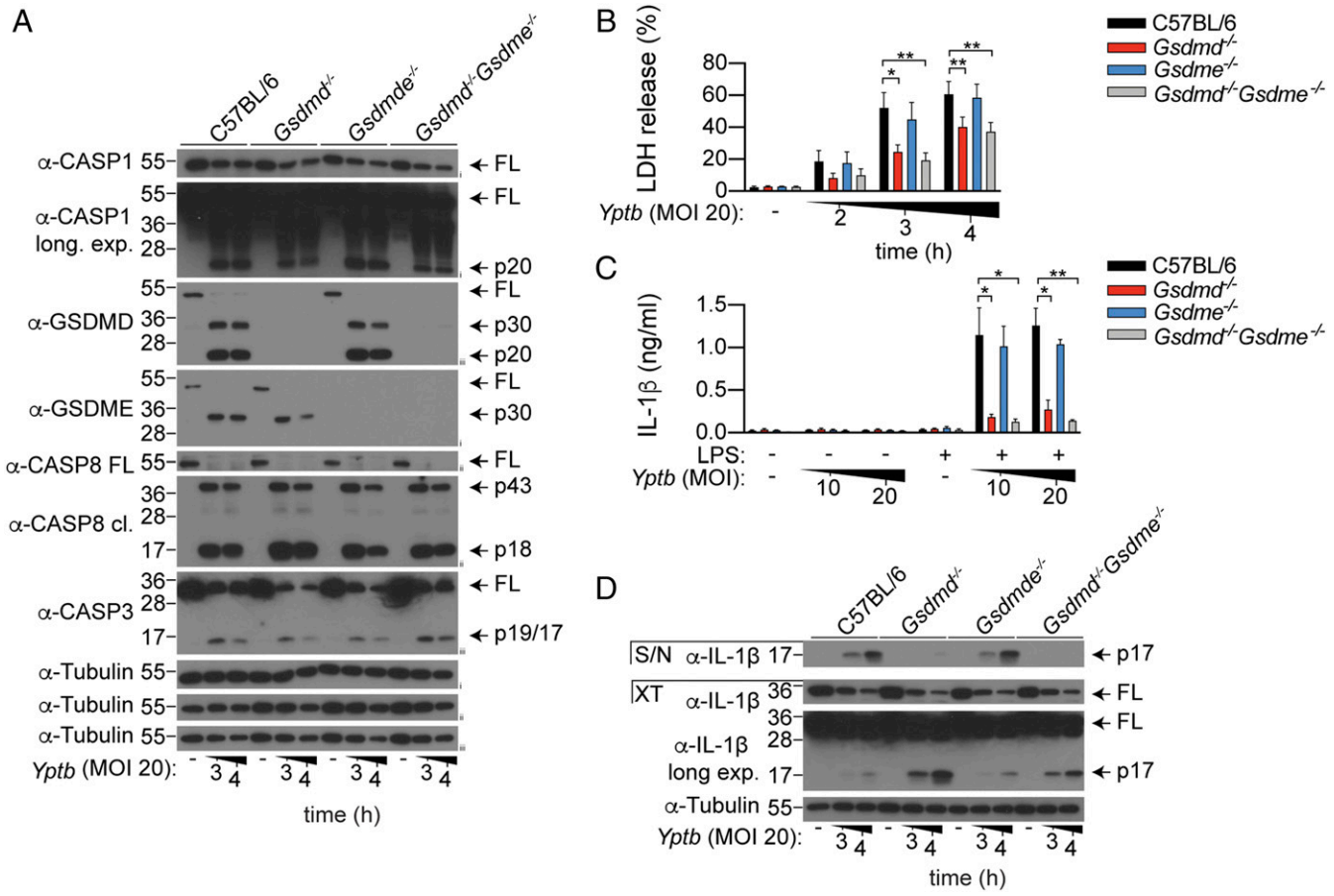

Fig. 2. GSDME is dispensable for macrophage pyroptosis and cytokine secretion upon *Yptb* infection. (*A* and *B*) Unprimed or (*C* and *D*) LPS-primed BMDMs were infected with *Yptb* for the (*A*, *B*, and *D*) indicated time points or (*C*) for 3 h. (*A*) Mixed supernatant and cell extracts were examined by immunoblotting. (*A–D*) Immunoblots are representative of three independent experiments. (*B* and *C*) Data are mean + SEM of pooled data from four independent experiments. $*P < 0.05$, $**P < 0.01$.

In keeping with this, we observed that GSDMD, but not GSDME, is required for IL-1β secretion from *Yptb*-infected BMDMs (Fig. 2 *C* and *D*). Collectively, these data indicate that while GSDME is processed into its p30 active fragment during *Yptb* infection, it is dispensable for macrophage pyroptosis and cytokine secretion.

GSDME, but not GSDMD, Promotes Apoptotic Neutrophil Cell Lysis.

Neutrophils play an important role in host defense against *Yersinia* infection (29, 30) and are the most abundant cell type that are injected with effector proteins during *Yersinia* infection (31). Therefore, we next examined the contribution of GSDMD and GSDME to neutrophil cell lysis and cytokine secretion following *Yptb* infection. Under in vitro conditions, unstimulated neutrophils undergo spontaneous activation of the intrinsic apoptosis pathway and progress into lytic cell death through an ill–defined mechanism (32). Surprisingly, while purifying bone marrow neutrophils for *Yersinia* infection, we observed that naïve *Gsdme*$^{-/-}$ neutrophils were significantly protected from spontaneous cell lysis, as uptake of the membrane-impermeable nucleic acid dye, propidium iodide (PI), was significantly reduced in *Gsdme*$^{-/-}$ neutrophils compared to WT controls (Fig. 3*A*). By contrast, PI uptake between WT and *Gsdmd*$^{-/-}$ neutrophils was indistinguishable (Fig. 3*A*), consistent with previous reports (7, 16, 19, 33). *Gsdmd*/*Gsdme* double deficiency did not further reduce PI uptake compared to *Gsdme*$^{-/-}$ neutrophils (Fig. 3*A*). The pan-caspase inhibitor, Q-VD-Oph (QVD), suppressed caspase-3 and GSDME activation in unstimulated neutrophils (Fig. 3*B*) and triggered a corresponding reduction in PI uptake compared to unstimulated WT and *Gsdmd*$^{-/-}$ neutrophils (Fig. 3*C*). QVD did not further reduce PI uptake in *Gsdme*$^{-/-}$ and *Gsdmd*$^{-/-}$*Gsdme*$^{-/-}$ neutrophils compared to unstimulated cells (Fig. 3*D*). In line with a previous report (21), we did not detect any difference in bone marrow or circulating neutrophil between naïve WT and *Gsdme*$^{-/-}$ animals in vivo (*SI Appendix*, Fig. S1 *A* and *B*). Collectively, these data demonstrate that GSDME is the major driver of spontaneous neutrophil lysis in vitro but does not regulate neutrophil turnover in naïve animals, since *Gsdme* deficiency does not block neutrophil apoptosis but rather reroutes it to a different outcome.

We next investigated whether GSDME drives neutrophil lysis following activation of extrinsic and intrinsic apoptosis. For this, we exposed neutrophils to TNF plus SMAC mimetic (SM) or FasL to induce extrinsic apoptosis, or ABT-737, plus S63845 to induce intrinsic apoptosis. Both extrinsic and intrinsic apoptosis triggered robust caspase-3 and GSDME activation (Fig. 3 *E* and *F*) and corresponding GSDME-dependent cell permeability and lysis, as measured by PI uptake and LDH release, respectively (Fig. 3 *G–J*). In contrast, *Gsdmd* deficiency did not impact PI uptake and LDH release in WT or *Gsdme*$^{-/-}$ neutrophils (Fig. 3 *G–J*). Next, we stimulated neutrophils with LPS, SM and QVD (LSQ) to induce RIPK3-dependent necroptosis (*SI Appendix*, Fig. S2 *A* and *B*) (34). As anticipated, PI uptake and LDH release between WT and *Gsdme*$^{-/-}$ neutrophils were comparable after LSQ stimulation (Fig. 3 *K* and *L*), indicating that *Gsdme*$^{-/-}$ neutrophils are

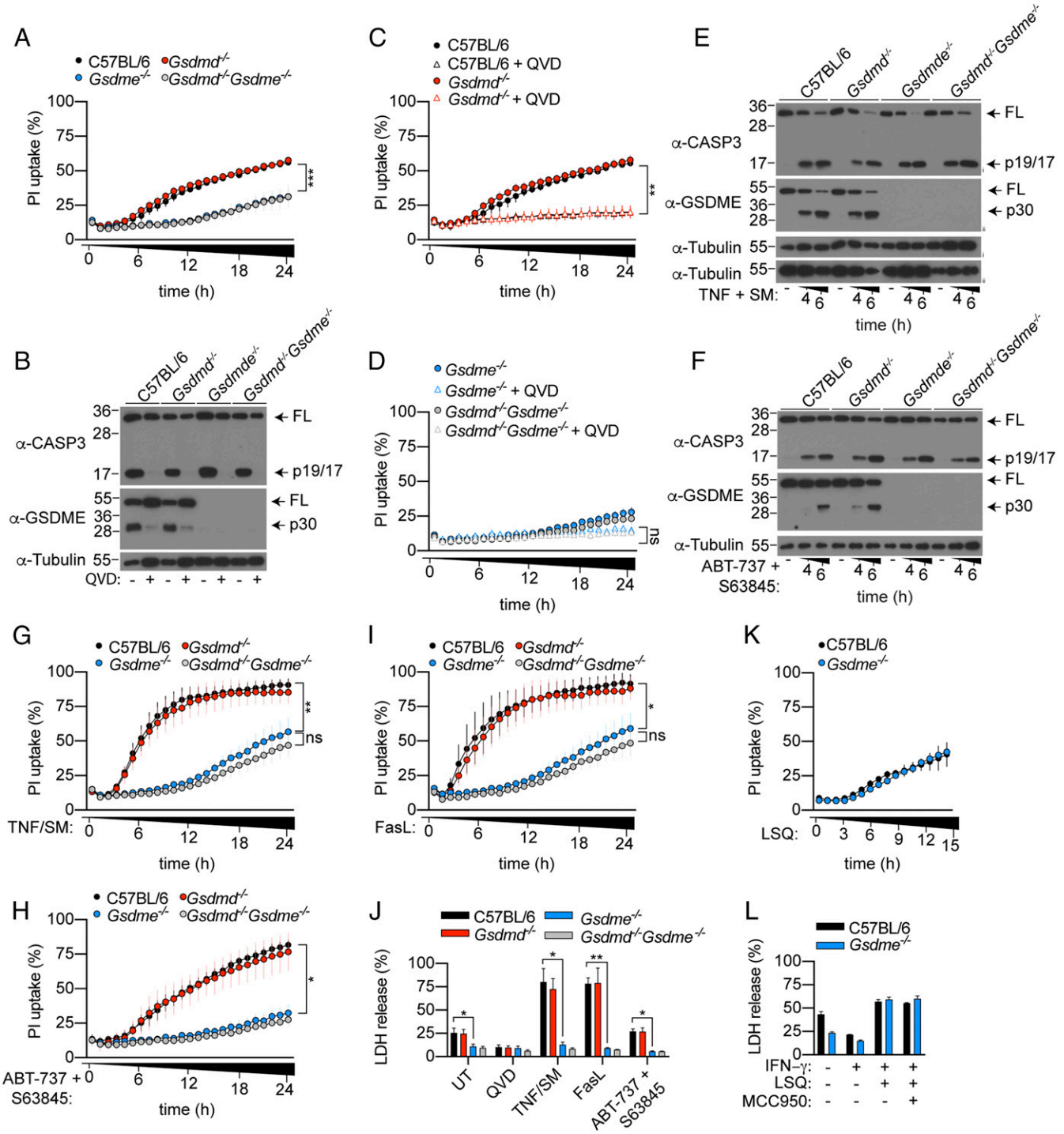

Fig. 3. GSDME activation is required for neutrophil lysis upon apoptotic caspase activation. (*A*, *C*, *D*, *G–I*, and *K*) PI uptake was quantified over 15 to 24 h. (*B*, *E*, and *F*) Mixed supernatant and cell extracts were examined by immunoblotting, representative of three independent experiments. (*J* and *K*) LDH release was measured at (*J*) 6 or (*L*) 15 h poststimulation. Data are mean + SEM pooled from three (*A*, *C*, *D*, *H*, and *J*) or four (*G* and *I*) independent experiments. (*K* and *L*) Data are mean + SD for technical triplicates representative from three independent experiments. $*P < 0.05$, $**P < 0.01$, $***P < 0.001$.

not intrinsically resistant to cell lysis. Collectively, this indicates that GSDME, but not GSDMD, promotes cellular lysis in apoptotic neutrophils.

GSDME Drives Neutrophil Pyroptosis upon *Yersinia* Infection.

We next sought to characterize the role of neutrophil GSDMD and GSDME during *Yptb* infection. We first primed neutrophils with IFN-γ in order to reduce spontaneous cell lysis (35) (*SI Appendix*, Fig. S3 *A* and *B*) and LPS to induce pro-IL-1β expression, prior to *Yptb* infection. Indeed, *Yptb* infection triggered GSDME-dependent neutrophil pyroptosis (Fig. 4*A*) and corresponding GSDME cleavage (Fig. 4*B*), which is dependent on the bacterial effector YopJ and RIPK1 kinase activity (*SI Appendix*, Fig. S3*C*). By contrast, GSDMD was dispensable on its own and did not further contribute to lysis in the absence of GSDME (Fig. 4*A*). Since GSDMD activation does not universally trigger pyroptosis in neutrophils (16, 33, 36, 37), we

next investigated the cleavage status of neutrophil GSDMD upon *Yptb* infection. WT and *Caspase-1/11*$^{-/-}$ neutrophils were challenged with *Yptb* or a *Salmonella ΔsifA* mutant, which triggers robust caspase-11–dependent GSDMD cleavage, as a positive control (16). In keeping with previous reports (16, 37), we observed robust processing of full-length GSDMD into the active p30 fragment upon caspase-11 activation in WT neutrophils (Fig. 4*C*). By contrast, GSDMD processing into the active p30 fragment was significantly weaker upon *Yptb* infection, while the inactive p43 and p20 species were more abundant (Fig. 4*C*) (8, 38). This suggests that in neutrophils, apoptotic caspases inactivate GSDMD during *Yptb* infection. In keeping with macrophage studies (11, 12), GSDMD processing was sensitive to the RIPK1 kinase inhibitor Nec-1s and only partially reduced in *Caspase-1/11*$^{-/-}$ neutrophils compared to WT controls upon *Yptb* infection (Fig. 4*C*). These data demonstrate that while both caspase-1 and -8 promote GSDMD processing, neutrophil pyroptosis upon *Yptb* infection is solely driven by GSDME.

Since GSDME overexpression sensitizes apoptotic tumor cells to GSDME-dependent pyroptosis (21), we next wondered whether GSDME expression correlates with susceptibility of myeloid cells to GSDME-dependent pyroptosis. To examine this possibility, we cultured equal numbers of macrophages and neutrophils as previously described (16, 39) and compared protein levels of GSDME in naïve and *Yptb*-infected cells by immunoblot. Unexpectedly, expression of full-length and cleaved GSDME were similar, if not slightly higher, in macrophages compared to neutrophils (Fig. 4*D*). This indicates that the resistance of macrophages or susceptibility of neutrophils to GSDME pores are not simply due to differential GSDME expression, in contrast to tumor cells (21).

GSDME-Dependent IL-1β Release Drives Host Defense against *Yersinia*.

Since *Yptb* is an extracellular bacterium and caspase-11–driven activation of GSDMD promotes the release of antimicrobial NETs (16), we examined whether GSDME activation also triggers NET extrusion to restrict *Yptb* replication in vitro. Interestingly, while *Yptb* infection triggered robust GSDME processing and pyroptosis (Fig. 4 *A* and *B*), it did not result in any hallmarks of NETosis including nuclear delobuation, expansion, or the appearance of diffused or spread NETs (Fig. 5 *A* and *B*) (14). Instead, *Yptb* infection triggered morphological hallmarks of pyroptosis, including membrane ballooning and nuclear condensation in a GSDME-dependent manner (Fig. 5*A*), indicating that GSDME activation does not promote NET extrusion. In support of this, WT and *Gsdme*$^{-/-}$ neutrophils killed *Yptb* to the same extent in vitro (Fig. 5*C* and *SI Appendix*, Fig. S4 *A–D*). Since GSDME activation does not appear to directly restrict bacterial growth and given that apoptotic signaling promotes IL-1β secretion from neutrophils (34, 40), we investigated whether GSDME activation drives the release of leaderless cytokines from pyroptotic neutrophils. In keeping with the cell lysis data (Fig. 4*A*), IL-1β release from *Yptb*-infected neutrophils was indeed GSDME dependent but GSDMD independent (Fig. 5*D*). Interestingly, while *Yptb* infection triggered caspase-1–dependent IL-1β maturation in macrophages (27), application of the NLRP3-specific inhibitor MCC950 or *caspase-1/11* deficiency had no impact on GSDME-dependent IL-1β secretion from neutrophils (Fig. 5 *D–F*). Instead, IL-1β cleavage requires RIPK1 kinase activity (Fig. 5*F*), indicating that IL-1β maturation is largely caspase-8 dependent in apoptotic neutrophils, consistent with our previous findings (34). In contrast, other leaderless IL-1 family

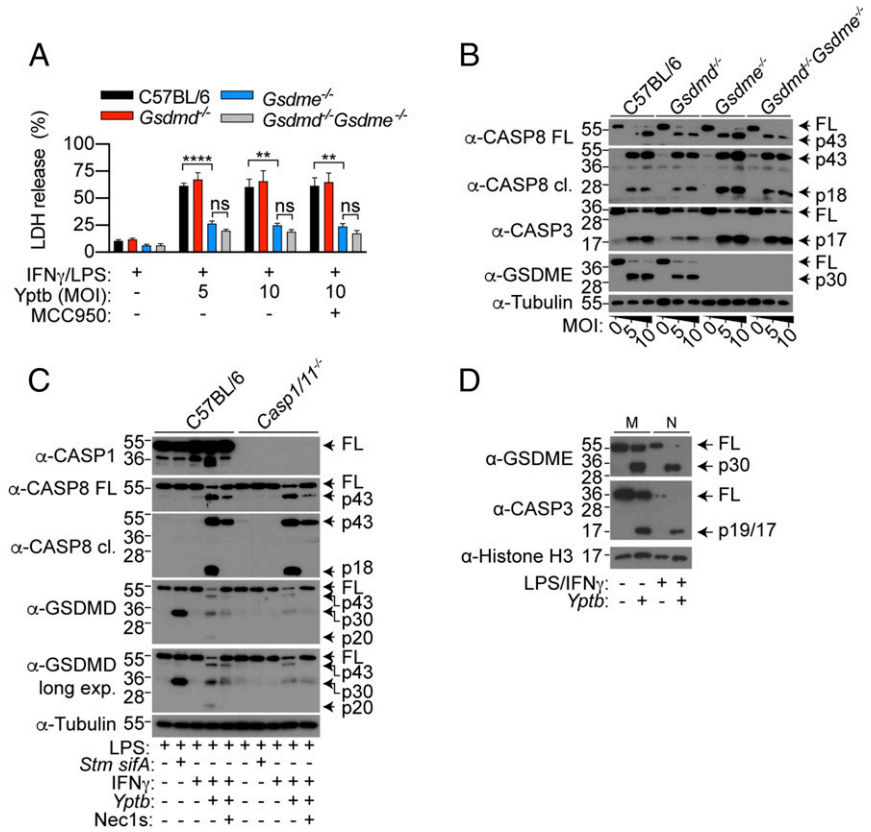

Fig. 4. *Yersinia* infection triggers GSDME-dependent cell death in neutrophils. (*A–D*) Neutrophils were infected with *Yptb* or *Salmonella ΔsifA* (both MOI 10) for 4 h. (*B–D*) Mixed supernatant and cell extracts were examined by immunoblotting, representative of three independent experiments. (*A*) Data are mean + SEM pooled from four independent experiments. $^{**}P < 0.01$, $^{****}P < 0.0001$.

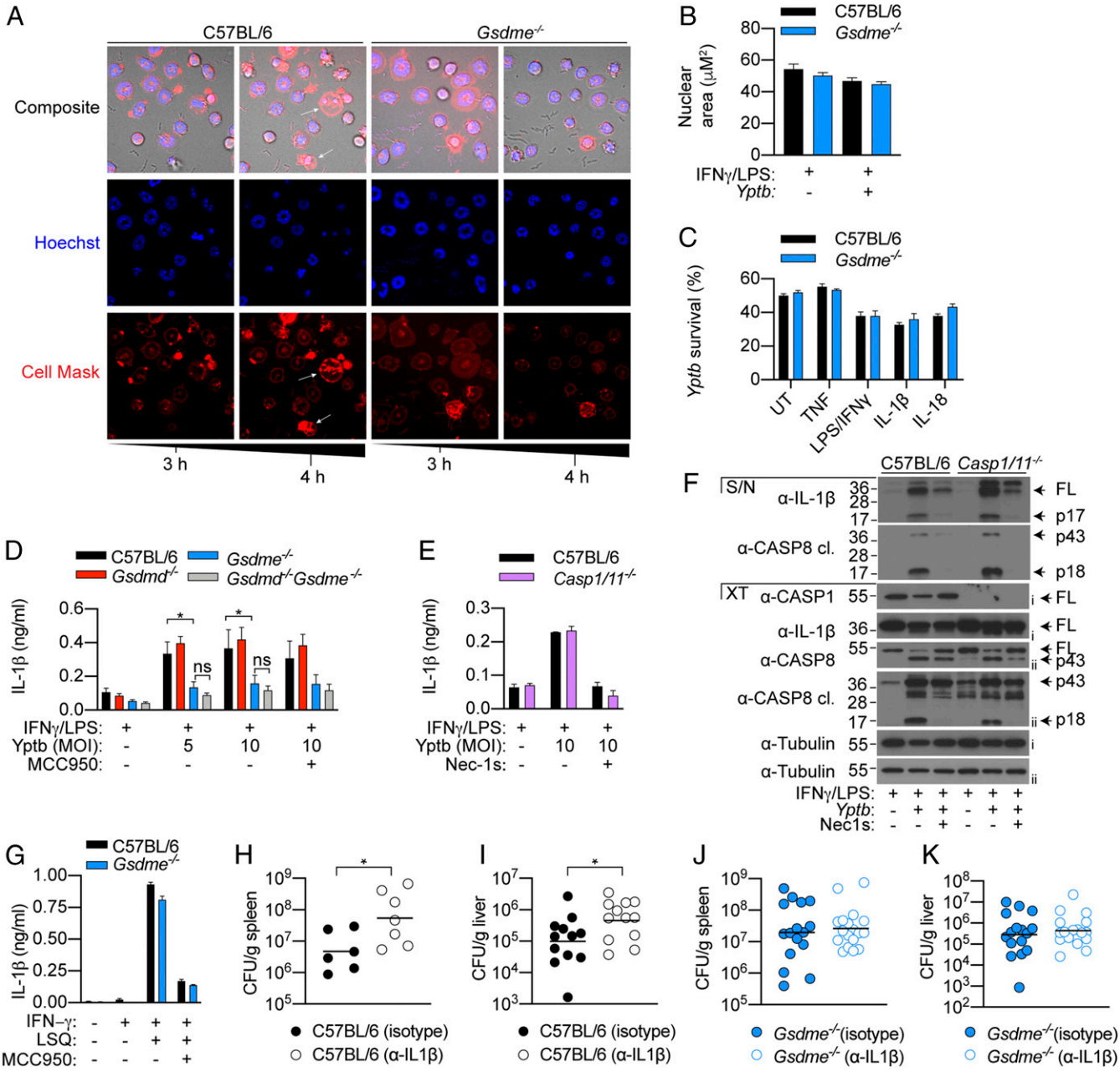

Fig. 5. GSDME-dependent IL-1β release promotes anti-*Yersinia* defense. (*A*) Time-lapse confocal images of *Yptb*-infected neutrophils (MOI 10). (*B*) Neutrophils were infected with *Yptb* (MOI 10) for 4 h and nuclear areas were quantified. (*C*) Neutrophils were left unstimulated or primed with the indicated cytokines or PAMPs for 2 h prior to *Yptb* (MOI 1) infection for 3 h in antibiotic-free media. *Yptb* survival relative to inoculum is displayed. (*D–F*) Neutrophils were infected with *Yptb* (MOI 10) for 4 h. (*F*) Precipitated supernatant and cell extracts were examined separately by immunoblotting, representative of two independent experiments. (*G*) Neutrophils were treated with LSQ for 15 h. (*H–K*) Mice were administered with isotype control or α-IL-1β neutralizing and challenged with *Yptb* for 5 d. Data are mean + SEM pooled from (*B*) five or (*D*) four independent experiments, (*C*, *E*, and *G*) + SD of triplicate stimulation representative of three independent experiments, or (*H–K*) geometric mean of pooled from two independent experiments. *$P < 0.05$.

cytokines, including IL-1α and IL-33, were barely detected in the supernatant of pyroptotic neutrophils (*SI Appendix*, Fig. S5 *A* and *B*). To ensure that the observed defect in IL-1β secretion is not due to a general secretion defect by *Gsdme*$^{-/-}$ neutrophils, we stimulated IFNγ-primed neutrophils with a combination of LSQ to induce necroptosis and subsequent NLRP3–caspase-1 activation (34, 41). As anticipated, IL-1β secretion from necroptotic neutrophils is sensitive to the NLRP3-specific inhibitor MCC950 and occurred independently of GSDME (Fig. 5*G*), confirming that *Gsdme*$^{-/-}$ neutrophils are not intrinsically defective in IL-1β release.

Since neutrophils are a major cellular source of IL-1β during various bacterial infection (36, 42, 43), we investigated whether GSDME promotes host resistance against *Yptb* by driving IL-1β release. Indeed, IL-1β neutralization triggered a significant increase in bacterial burden in the spleen and liver of WT animals compared to isotype control (Fig. 5 *H* and *I*), while the same regimen had no impact on bacterial clearance in *Gsdme*$^{-/-}$ animals (Fig. 5 *J* and *K*). These observations indicate that GSDME and likely neutrophils are the major cellular source of IL-1β during *Yptb* infection. In agreement with this, we detected significantly lower plasma IL-1β in neutropenic

Genista animals (44) compared to WT controls upon *Yptb* infection (*SI Appendix*, Fig. S6 *A* and *B*). Collectively, these data reveal an unexpected role of neutrophil GSDME as a major cellular driver of IL-1β release during *Yersinia* infection.

Discussion

The discovery of the gasdermin protein family has greatly revolutionized our understanding of cell death during microbial infection. However, the majority of studies focused solely on the archetypal gasdermin, GSDMD, for which a host of exciting functions including cytokine secretion (17–19), NET extrusion (14, 16), and repression of cGAS signaling (45) were described. By contrast, the physiological function of GSDME during microbial infection is unclear. In this study, we report that GSDME is a potent antimicrobial effector that defends against blockade of innate immune signaling by the Gram-negative bacterium *Yptb*. Unexpectedly, we found that GSDME exerts its antimicrobial function in neutrophils by driving cellular pyroptosis and bioactive IL-1β release from YopJ-injected cells. Although neutrophils were once regarded as effector cells that contribute minimally to orchestrate the immune response, this view is rapidly evolving as an increasing number of studies now document neutrophils as a major cellular source of proinflammatory cytokines (e.g., IL-1β and IL-8) during microbial infection (36, 42, 43, 46). Our study agrees with such a model, as we found that neutralization of IL-1β impaired bacterial clearance in WT, but not *Gsdme*$^{-/-}$, animals, indicating that GSDME pores, and likely neutrophils, are a major cellular source of IL-1β during *Yersinia* infection. Since RIPK1 kinase activity in myeloid cells drives anti-*Yersinia* defense (24), it is possible that GSDME may also promote pyroptosis and bioactive IL-1β release from infected inflammatory monocytes. Given that gasdermin cleavage elicits distinct functional outcomes in different myeloid cell subsets (16, 33, 36, 37), future studies characterizing the regulation and biological function of gasdermins in monocytes will be of interest. One potential caveat of our study, however, is the sensitivity between murine and human myeloid cells to *Yersinia* infection. While pathogenic *Yersinia* are often used to study cell death and gasdermin function in murine systems, human macrophages and neutrophils appear to be much more resistant to YopJ or small-molecule TAK1 inhibitor–induced cell death compared to their murine counterparts (12, 47). This difference likely reflects higher expression of prosurvival molecules such as FADD-like IL-1β-converting enzyme (FLICE) inhibitor protein (FLIP) in human myeloid cells (48).

Overexpression of GSDME in tumor cells or immortalized macrophages sensitizes cells to GSDME-dependent pyroptosis (21, 49); this observation has led to the assumption that GSDME expression determines the sensitivity of a given cell to pyroptosis. Surprisingly, we found no evidence that GSDME promotes pyroptosis or IL-1β secretion in macrophages during *Yersinia* infection, despite expressing equal or more GSDME than pyroptosis-competent neutrophils on a per cell basis. This makes intuitive sense, as we recently reported that caspase-3 and 7 promote anti-*Yersinia* defense in vivo by cleaving and inactivating GSDMD at position aspartate 88 (27). Since GSDME is also dispensable for chemotherapy-induced macrophages lysis (8), it is unlikely that the lack of GSDME-dependent macrophage pyroptosis is driven by a pathogen subversion mechanism. As caspase-3 and 7 were reported to inactivate innate immune signaling pathways in apoptotic cells (50, 51), it is tempting to speculate that caspase-3 and 7 likewise initiates a membrane repair mechanism to suppress GSDME-driven pyroptosis in macrophages, as we previously described for GSDMD pores (52).

Our discovery that GSDME promotes neutrophil lysis and bioactive IL-1β release has major implications beyond infectious disease, as these processes are implicated in a variety of human diseases. For example, aberrant IL-1β secretion is associated with atherosclerosis, diabetes, neurological diseases, gout, and rheumatoid arthritis. Because IL-1β secretion is significantly reduced in *Gsdmd*-deficient macrophages, GSDMD inhibitors are now regarded as attractive therapeutical targets for IL-1β–mediated disease. Our finding that GSDME promotes mature IL-1β release during in vivo infection unravels a previously unappreciated role for other gasdermins in driving IL-1β secretion. Future studies investigating the contribution of GSDME to such diseases may uncover therapeutics.

Materials and Methods

Animals. All experiments involving animals were performed under the guidelines and approval from the Swiss animal protection law (license VD3257) and guidelines from the NIH and the University of Pennsylvania Institutional Animal Use and Care Committee (Protocol 804523). C57BL/6J, *Ripk1*$^{D138N/D138N}$ *Gsdmd*$^{-/-}$, *Gsdme*$^{-/-}$, *Gsdmd*$^{-/-}$*Gsdme*$^{-/-}$, *Casp1/11*$^{-/-}$, and *Genista* (all either generated in or back-crossed to the C57BL/6 background) were previously described (8, 44, 53) and housed in specific pathogen–free facilities at the University of Lausanne. An independent line of *Gsdme*$^{-/-}$ was generated at the University of Pennsylvania. *Gsdme* was knocked out in the C57BL/6J background by targeting exons 2 and 3 using two CRISPR gRNAs (CAGAACCCTCCTGTCACGAT and TGTGATATGGAGTACCCCGA) as previously described (54). Briefly, eggs were microinjected with the two gRNAs along with Cas9 mRNA. Progeny were screened for successful deletion, and successfully deleted males were bred to C57BL/6J females. Germ-line–transmitted founders were intercrossed to establish the *Gsdme*$^{-/-}$ line.

Primary Myeloid Cell Culture. BMDMs were differentiated in Dulbecco's modified Eagle medium (Gibco) containing 20% 3T3 supernatant (as a source of M-CSF), 10% heat-inactivated fetal calf serum (Bioconcept), 10 mM Hepes (Bioconcept), penicillin/streptomycin (Bioconcept), and nonessential amino acids (Gibco) and stimulated on days 7 to 9 of differentiation. Mature neutrophils were purified from murine bone marrow using anti-Ly6G-FITC (1A8 clone) and anti-FITC beads (Miltenyi) (>98% purity) as previously described (36). In all experiments, neutrophils were seeded at a density of 4×10^5 cells per well in 200 μl Opti-MEM and stimulated on the day of purification, and macrophages were seeded at a density of 5×10^4 cells per well in complete media a day prior to stimulation.

Apoptosis and Necroptosis Assay. To activate extrinsic apoptosis, neutrophils were stimulated with recombinant murine TNF (100 ng/mL; Peprotech) and the SMAC mimetic AZD 5582 (0.25 μM; Selleckchem) or 100 ng/mL Fc-Fas (kind gift from Prof Pascal Schneider; University of Lausanne). To activate intrinsic apoptosis, neutrophils were stimulated with ABT-737 (500 nM; Selleckchem) and S63845 (500 nM; Selleckchem). To induce neutrophil necroptosis, cells were primed with recombinant murine IFN-γ (100 ng/mL; Peprotech) for 1 h, followed by 2 h incubation with *Escherichia coli* 055:B5 LPS (100 ng/mL; Invivogen). Cells were treated with 10 μM Q-VD-Oph in the last 20 to 30 min of LPS priming and stimulated with the SMAC mimetic AZD 5582 (0.25 μM; Selleckchem). Where indicated, neutrophils were treated with the NLRP3-specific inhibitor MCC950 (10 μM; Invivogen) 20 min before SMAC mimetic treatment.

***Yersinia* Infection.** Where indicated, macrophages were primed with *E. coli* 055:B5 LPS (100 ng/mL; Invivogen) for 3 h prior to infection. For neutrophil infection, cells were coprimed with IFN-γ (100 ng/mL; Peprotech) and *E. coli* 055:B5 LPS (100 ng/mL; Invivogen) for 3 h prior to infection. Log-phase *Yptb* strain 32777 were prepared and used to infect BMDM or neutrophils at a multiplicity of infection (MOI) 5 to 20 as previously described (27). IL-1α, IL-1β, and IL-33 levels in cell-free supernatant were measured by enzyme-linked immunosorbent assay (ELISA) according to manufacturers' instruction (all R&D Systems DuoSet ELISA). For in vivo infection, mice were fasted for 16 h and challenged with 2×10^8 CFU stationary-phase bacteria by oral gavage. To determine bacterial burden, mice were euthanized 4 or 5 d postinfection and tissues were harvested, homogenized in 1 mL of phosphate-buffered saline, and serially diluted on Luria–Bertani (LB) agar.

***Salmonella* Infection.** Mature neutrophils were seeded at a density of 4×10^5 cells per well in 200 μl Opti-MEM and primed with *E. coli* 055:B5 LPS (100 ng/mL; Invivogen) for 3 h. *Salmonella enterica* serovar Typhimurium SL1344 Δ*sifA* mutant were grown overnight with aeration at 37 °C in LB media, and stationary-phase bacteria were used to infect neutrophils as previously described (16).

Cell Death Measurements. Cell permeabilization was quantified by measuring PI (1 μg/mL; Thermo Fisher Scientific) uptake over time using a fluorescent plate reader (Cytation5; Biotek). Cell lysis was quantified by measuring the amount of intracellular LDH release into the cell culture supernatant (TaKaRa LDH cytotoxicity detection kit; Clontech). Percentage PI uptake and LDH release were calculated relative to 100% cell lysis in untreated control sample.

Immunoblotting. Cell culture supernatants were precipitated with methanol and chloroform using standard methods and resuspended in cell extracts lysed in boiling lysis buffer (66 mM Tris-Cl [pH 7.4], 2% SDS, 10 mM DTT, NuPage LDS sample buffer; Thermo Fisher). Proteins were separated on 14% polyacrylamide gels and transferred onto nitrocellulose membrane using Transblot Turbo (Bio-Rad). Antibodies for immunoblot were against GSDME (EPR19859; Abcam; 1:1,000), GSDMD (EPR19828; Abcam; 1:3,000), full-length caspase-8 (4927; Cell Signaling Technology ; 1:1,000), cleaved caspase-8 (9429; Cell Signaling Technology ; 1:1,000), caspase-3 (9662; Cell Signaling Technology ; 1:1,000), caspase-1 p20 (casper-1; Adipogen; 1:1,000), pro-IL-1β (AF-401-NA; R&D; 1:1,000), histone H3 (96C10; Cell Signaling Technology; 1:1,000), and alpha-tubulin (DM1A; Abcam; 1:5,000).

Imaging. Neutrophils were seeded in 8-well tissue culture–treated μ-Slides (ibidi) tissue culture plates and infected as described above. Images on μ-Slides (ibidi) were taken every hour using a Zeiss LSM800 point scanning confocal microscope equipped with 63× Plan-Apochromat NA 1.4 oil objective, Zeiss ESID detector module, LabTek heating/CO_2 chamber, and motorized scanning stage. Alternatively, neutrophils were seeded on 0.0001% poly-L-lysine–coated glass coverslips and fixed in 2% PFA for 15 min. Coverslips were stained with 4′,6-diamidino-2-phenylindole (DAPI). Nuclear area were quantified using the automated Gen5 Imaging software (BioTek).

Flow Cytometry. Bone marrow cells were blocked with TruStain FcX (anti-mouse CD16/32; Biolegend) and stained with CD11b (M1/70; Biolegend) and Ly6G (1A8; Biolegend) to identify neutrophil population. Blood neutrophils were identified as $CD45.2^+$ (104; Biolegend) $Gr\text{-}1^+$ (RB6-8C5; Biolegend) SSC^{high} cells or stained with LIVE/DEAD Fixable Aqua Dead Cell Stain Kit (Invitrogen) and identified as $CD11b^+$ (M1/70; Biolegend) $Ly6G^+$ (1A8; Biolegend) cells. Cell profiles were acquired using BD Accuri C6 Plus and Fortessa I, as well as Cytek Aurora, and analyzed using FlowJo (Tree Star).

Statistical Analyses. Statistical analyses were performed using Prism 8 (Graphpad) software. Parametric *t* test was used for normally distributed data sets, while nonnormally distributed data sets were analyzed using nonparametric Mann-Whitney *t* tests. For PI uptake, area under the curve was calculated for each sample, and pooled data from three to four independent experiments were analyzed using a one-way ANOVA. Survival curves were compared using log–rank Mantel–Cox test. Data were considered significant when $P \leq 0.05$.

Data Availability. All study data are included in the article and/or *SI Appendix*.

ACKNOWLEDGMENTS. We thank Prof. Manolis Pasparakis (University of Cologne, Germany) and Prof. Pascal Schneider (University of Lausanne) for generously providing *Ripk1*$^{D138N/D138N}$ mice and Fc-FasL, respectively. We thank Dr. Romain Bedel and Dr. Anne Wilson (University of Lausanne) for assistance on flow cytometry and Dr. Lance Peterson (Washington University in St. Louis) for discussion. This work was supported by a European Research Council Grant (ERC2017-CoG-770988-InflamCellDeath) and Swiss National Science Foundation Project Grants (310030_175576 and 310030B_198005) to P.B., a National University of Singapore Start Up Grant and a Ministry of Education Inauguration Grant to K.W.C., a Mark Foundation Grant (19-011MIA) and NIH Grant (R01-139102) to I.E.B., and a Swiss National Science Foundation Grant (310030_184751) to F.T.-C.

1. J. Shi, W. Gao, F. Shao, Pyroptosis: Gasdermin-mediated programmed necrotic cell death. *Trends Biochem. Sci.* **42**, 245–254 (2017).
2. P. Broz, P. Pelegrín, F. Shao, The gasdermins, a protein family executing cell death and inflammation. *Nat. Rev. Immunol.* **20**, 143–157 (2020).
3. R. A. Aglietti *et al*., GsdmD p30 elicited by caspase-11 during pyroptosis forms pores in membranes. *Proc. Natl. Acad. Sci. U.S.A.* **113**, 7858–7863 (2016).
4. J. Ding *et al*., Pore-forming activity and structural autoinhibition of the gasdermin family. *Nature* **535**, 111–116 (2016).
5. X. Liu *et al*., Inflammasome-activated gasdermin D causes pyroptosis by forming membrane pores. *Nature* **535**, 153–158 (2016).
6. L. Sborgi *et al*., GSDMD membrane pore formation constitutes the mechanism of pyroptotic cell death. *EMBO J.* **35**, 1766–1778 (2016).
7. S. S. Burgener *et al*., Cathepsin G inhibition by Serpinb1 and Serpinb6 prevents programmed necrosis in neutrophils and monocytes and reduces GSDMD-driven inflammation. *Cell Rep.* **27**, 3646–3656.e5 (2019).
8. K. W. Chen *et al*., Extrinsic and intrinsic apoptosis activate pannexin-1 to drive NLRP3 inflammasome assembly. *EMBO J.* **38**, e101638 (2019).
9. H. Kambara *et al*., Gasdermin D exerts anti-inflammatory effects by promoting neutrophil death. *Cell Rep.* **22**, 2924–2936 (2018).
10. N. Kayagaki *et al*., Caspase-11 cleaves gasdermin D for non-canonical inflammasome signalling. *Nature* **526**, 666–671 (2015).
11. P. Orning *et al*., Pathogen blockade of TAK1 triggers caspase-8-dependent cleavage of gasdermin D and cell death. *Science* **362**, 1064–1069 (2018).
12. J. Sarhan *et al*., Caspase-8 induces cleavage of gasdermin D to elicit pyroptosis during *Yersinia* infection. *Proc. Natl. Acad. Sci. U.S.A.* **115**, E10888–E10897 (2018).
13. J. Shi *et al*., Cleavage of GSDMD by inflammatory caspases determines pyroptotic cell death. *Nature* **526**, 660–665 (2015).
14. G. Sollberger, D. O. Tilley, A. Zychlinsky, Neutrophil extracellular traps: The biology of chromatin externalization. *Dev. Cell* **44**, 542–553 (2018).
15. I. Jorgensen, Y. Zhang, B. A. Krantz, E. A. Miao, Pyroptosis triggers pore-induced intracellular traps (PITs) that capture bacteria and lead to their clearance by efferocytosis. *J. Exp. Med.* **213**, 2113–2128 (2016).
16. K. W. Chen *et al*., Noncanonical inflammasome signaling elicits gasdermin D-dependent neutrophil extracellular traps. *Sci. Immunol.* **3**, eaar6676 (2018).
17. C. L. Evavold *et al*., The pore-forming protein gasdermin D regulates interleukin-1 secretion from living macrophages. *Immunity* **48**, 35–44.e6 (2018).
18. M. Monteleone *et al*., Interleukin-1β maturation triggers its relocation to the plasma membrane for gasdermin-D-dependent and -independent secretion. *Cell Rep.* **24**, 1425–1433 (2018).
19. R. Heilig *et al*., The gasdermin-D pore acts as a conduit for IL-1β secretion in mice. *Eur. J. Immunol.* **48**, 584–592 (2018).
20. A. H. Chan, K. Schroder, Inflammasome signaling and regulation of interleukin-1 family cytokines. *J. Exp. Med.* **217**, e20190314 (2020).
21. Y. Wang *et al*., Chemotherapy drugs induce pyroptosis through caspase-3 cleavage of a gasdermin. *Nature* **547**, 99–103 (2017).
22. Z. Zhang *et al*., Gasdermin E suppresses tumour growth by activating anti-tumour immunity. *Nature* **579**, 415–420 (2020).
23. C. Rogers *et al*., Cleavage of DFNA5 by caspase-3 during apoptosis mediates progression to secondary necrotic/pyroptotic cell death. *Nat. Commun.* **8**, 14128 (2017).
24. L. W. Peterson *et al*., RIPK1-dependent apoptosis bypasses pathogen blockade of innate signaling to promote immune defense. *J. Exp. Med.* **214**, 3171–3182 (2017).
25. N. H. Philip *et al*., Caspase-8 mediates caspase-1 processing and innate immune defense in response to bacterial blockade of NF-κB and MAPK signaling. *Proc. Natl. Acad. Sci. U.S.A.* **111**, 7385–7390 (2014).
26. D. Weng *et al*., Caspase-8 and RIP kinases regulate bacteria-induced innate immune responses and cell death. *Proc. Natl. Acad. Sci. U.S.A.* **111**, 7391–7396 (2014).
27. B. Demarco *et al*., Caspase-8-dependent gasdermin D cleavage promotes antimicrobial defense but confers susceptibility to TNF-induced lethality. *Sci. Adv.* **6**, eabc3465 (2020).
28. L. Wang, F. Du, X. Wang, TNF-alpha induces two distinct caspase-8 activation pathways. *Cell* **133**, 693–703 (2008).
29. J. Mecsas, Unraveling neutrophil- *Yersinia* interactions during tissue infection. *F1000Res.* **8**, F1000 Faculty Rev-1046 (2019).
30. L. Shaban *et al*., Yersinia pseudotuberculosis YopH targets SKAP2-dependent and independent signaling pathways to block neutrophil antimicrobial mechanisms during infection. *PLoS Pathog.* **16**, e1008576 (2020).
31. E. A. Durand, F. J. Maldonado-Arocho, C. Castillo, R. L. Walsh, J. Mecsas, The presence of professional phagocytes dictates the number of host cells targeted for Yop translocation during infection. *Cell. Microbiol.* **12**, 1064–1082 (2010).
32. B. A. Croker, A. W. Roberts, N. A. Nicola, Towards a four-dimensional view of neutrophils. *Methods Mol. Biol.* **844**, 87–99 (2012).
33. M. Karmakar *et al*., N-GSDMD trafficking to neutrophil organelles facilitates IL-1β release independently of plasma membrane pores and pyroptosis. *Nat. Commun.* **11**, 2212 (2020).
34. K. W. Chen *et al*., Cutting edge: Blockade of inhibitor of apoptosis proteins sensitizes neutrophils to TNF- but not lipopolysaccharide-mediated cell death and IL-1β secretion. *J. Immunol.* **200**, 3341–3346 (2018).
35. F. Colotta, F. Re, N. Polentarutti, S. Sozzani, A. Mantovani, Modulation of granulocyte survival and programmed cell death by cytokines and bacterial products. *Blood* **80**, 2012–2020 (1992).
36. K. W. Chen *et al*., The neutrophil NLRC4 inflammasome selectively promotes IL-1β maturation without pyroptosis during acute Salmonella challenge. *Cell Rep.* **8**, 570–582 (2014).
37. S. B. Kovacs *et al*., Neutrophil caspase-11 is essential to defend against a cytosol-invasive bacterium. *Cell Rep.* **32**, 107967 (2020).
38. C. Y. Taabazuing, M. C. Okondo, D. A. Bachovchin, Pyroptosis and apoptosis pathways engage in bidirectional crosstalk in monocytes and macrophages. *Cell Chem. Biol.* **24**, 507–514.e4 (2017).
39. D. Boucher *et al*., Caspase-1 self-cleavage is an intrinsic mechanism to terminate inflammasome activity. *J. Exp. Med.* **215**, 827–840 (2018).
40. S. Wicki *et al*., Loss of XIAP facilitates switch to TNFα-induced necroptosis in mouse neutrophils. *Cell Death Dis.* **7**, e2422 (2016).
41. S. A. Conos *et al*., Active MLKL triggers the NLRP3 inflammasome in a cell-intrinsic manner. *Proc. Natl. Acad. Sci. U.S.A.* **114**, E961–E969 (2017).

42. J. S. Cho *et al*., Neutrophil-derived IL-1β is sufficient for abscess formation in immunity against Staphylococcus aureus in mice. *PLoS Pathog.* **8**, e1003047 (2012).
43. M. Karmakar, Y. Sun, A. G. Hise, A. Rietsch, E. Pearlman, Cutting edge: IL-1β processing during Pseudomonas aeruginosa infection is mediated by neutrophil serine proteases and is independent of NLRC4 and caspase-1. *J. Immunol.* **189**, 4231–4235 (2012).
44. D. Ordoñez-Rueda *et al*., A hypomorphic mutation in the Gfi1 transcriptional repressor results in a novel form of neutropenia. *Eur. J. Immunol.* **42**, 2395–2408 (2012).
45. I. Banerjee *et al*., Gasdermin D restrains type I interferon response to cytosolic DNA by disrupting ionic homeostasis. *Immunity* **49**, 413–426.e5 (2018).
46. F. Bazzoni *et al*., Phagocytosing neutrophils produce and release high amounts of the neutrophil-activating peptide 1/interleukin 8. *J. Exp. Med.* **173**, 771–774 (1991).
47. J. L. Spinner *et al*., Neutrophils are resistant to Yersinia YopJ/P-induced apoptosis and are protected from ROS-mediated cell death by the type III secretion system. *PLoS One* **5**, e9279 (2010).
48. H. I. Muendlein *et al*., $cFLIP_L$ protects macrophages from LPS-induced pyroptosis via inhibition of complex II formation. *Science* **367**, 1379–1384 (2020).
49. B. Zhou, D. W. Abbott, Gasdermin E permits interleukin-1 beta release in distinct sublytic and pyroptotic phases. *Cell Rep.* **35**, 108998 (2021).
50. A. Rongvaux *et al*., Apoptotic caspases prevent the induction of type I interferons by mitochondrial DNA. *Cell* **159**, 1563–1577 (2014).
51. M. J. White *et al*., Apoptotic caspases suppress mtDNA-induced STING-mediated type I IFN production. *Cell* **159**, 1549–1562 (2014).
52. S. Rühl *et al*., ESCRT-dependent membrane repair negatively regulates pyroptosis downstream of GSDMD activation. *Science* **362**, 956–960 (2018).
53. A. Polykratis *et al*., Cutting edge: RIPK1 Kinase inactive mice are viable and protected from TNF-induced necroptosis in vivo. *J. Immunol.* **193**, 1539–1543 (2014).
54. J. Henao-Mejia *et al*., Generation of genetically modified mice using the CRISPR-Cas9 genome-editing system. *Cold Spring Harb. Protoc.* **2016**, pdb.prot090704 (2016).